2013

Broadening the Cloaking Bandwidth with Non-Foster Metasurfaces

Pai-Yen Chen
University of Texas at Austin

Christos Argyropoulos
University of Texas at Austin, christos.argyropoulos@unl.edu

Andrea Alu
University of Texas at Austin

Broadening the Cloaking Bandwidth with Non-Foster Metasurfaces

Pai-Yen Chen, Christos Argyropoulos, and Andrea Alù

The University of Texas at Austin, Department of Electrical and Computer Engineering, Austin, Texas 78712, USA

(Received 24 June 2013; published 3 December 2013)

We introduce the concept and practical design of broadband, ultrathin cloaks based on non-Foster, negatively capacitive metasurfaces. By using properly tailored, active frequency-selective screens conformal to an object, within the realm of a practical realization, we show that it is possible to drastically reduce the scattering over a wide frequency range in the microwave regime, orders of magnitude broader than any available passive cloaking technology. The proposed active cloak may impact not only invisibility and camouflaging, but also practical antenna and sensing applications.

DOI: 10.1103/PhysRevLett.111.233001 PACS numbers: 81.05.Xj, 42.50.Gy, 78.67.Pt

Metamaterials and plasmonic materials have attracted wide attention in recent years due to their exciting applications, which include the possibility of suppressing the visibility of an object by realizing suitably designed cloaking layers [1–10]. Beyond camouflaging, metamaterial cloaks have been proposed for noninvasive probing [11], high-fidelity biomedical measurements [12], low-noise communications [13], optical tagging [14], nonlinear nanodevices [15], and scattering signature manipulation [16]. The drastic suppression of an object's scattering is generally possible based on the anomalous wave interaction with artificially engineered metamaterials, provided that their material dispersion and spatial profiles meet the required theoretical requirements. Despite recent advances in metamaterial engineering [17], so far the practical realization of these devices has faced significant challenges, due to the stringent requirements on material properties and fundamental constraints on the overall bandwidth of operation. This problem is particularly evident for transformation-based cloaks [3–8], which inherently require extreme material properties, anisotropy, and inhomogeneity profiles. To meet these requirements, resonant and dispersive inclusions are necessary, implying severe bandwidth limitations and high sensitivity to disorder and imperfections. Solutions to relax these limitations have been suggested by reducing the requirement on maximum scattering suppression [18], but inherent limitations associated with causality and passivity appear to fundamentally limit the cloaking performance of any available technology that aims at suppressing the total scattering from an object in all directions and for all excitations [19–23].

Recently, we proposed and experimentally verified an alternative cloaking technique, named mantle cloaking [24–27], based on the concept of "cloaking by a surface," for which a suitably designed metasurface supports current distributions radiating "antiphase" fields that cancel the scattering from the covered object. Mantle cloaks can be readily realized at microwaves by patterning a metallic surface around the object of interest, and various structural designs [see Fig. 1(a)] have been proposed in the context of metasurfaces and frequency-selective surfaces (FSS) [28]. We have recently shown that even a one-atom-thick graphene monolayer may achieve scattering suppression at THz frequencies [29]. The ultrathin profile of mantle cloaks makes their practical realization easier than bulk metamaterial cloaks, and it is also usually associated with a moderate bandwidth improvement compared with the other cloaking techniques based on bulk metamaterials [24]. Still, similar bandwidth limitations apply to this scenario, and they are fundamentally related to the passivity of these designs [19]. Achieving broadband cloaks, on the contrary, may be disruptive for several of the above mentioned applications and may finally bring metamaterials close to a practical impact on technology.

In order to understand the fundamental limitations on bandwidth specifically applied to the mantle cloaking technique, consider the simple case of an infinite cylinder with relative permittivity $\varepsilon = 3$, relative permeability $\mu = 1$, and diameter $2a = 12$ cm, covered by a two-dimensional conformal mantle cloak with radius a_c [see Fig. 1(c)]. If the periodicity of the metallic patterns is smaller than the wavelength of operation, under certain symmetries of the excitation, we can describe the metasurface with an isotropic averaged surface impedance $Z_s = R_s - iX_s$ under an $e^{-i\omega t}$ time convention [24,26].

For a normally incident, transverse-magnetic (TM) plane wave with magnetic field polarized orthogonal to the cylinder axis [Fig. 1(c)], for which largest interaction is expected in the case of an object of moderate thickness, the Mie scattering coefficients may be written [24] as $c_n^{\mathrm{TM}} = -U_n^{\mathrm{TM}}/(U_n^{\mathrm{TM}} + iV_n^{\mathrm{TM}})$, and the total scattering width (SW) of the cylinder normalized to the wavelength, a quantitative measure of its overall visibility, becomes [30] $\sigma_{2\mathrm{D}} = \frac{2}{\pi}\sum_{n=0}^{n=\infty}(2 - \delta_{n,0})|c_n^{\mathrm{TM}}|^2$. In the long-wavelength limit, these expressions simplify, as the $n = 0$ harmonic dominates the overall scattering, and the condition to achieve identically zero c_0^{TM} becomes [25]

$$X_s = \frac{2}{\omega a \gamma \varepsilon_0(\varepsilon - 1)}, \tag{1}$$

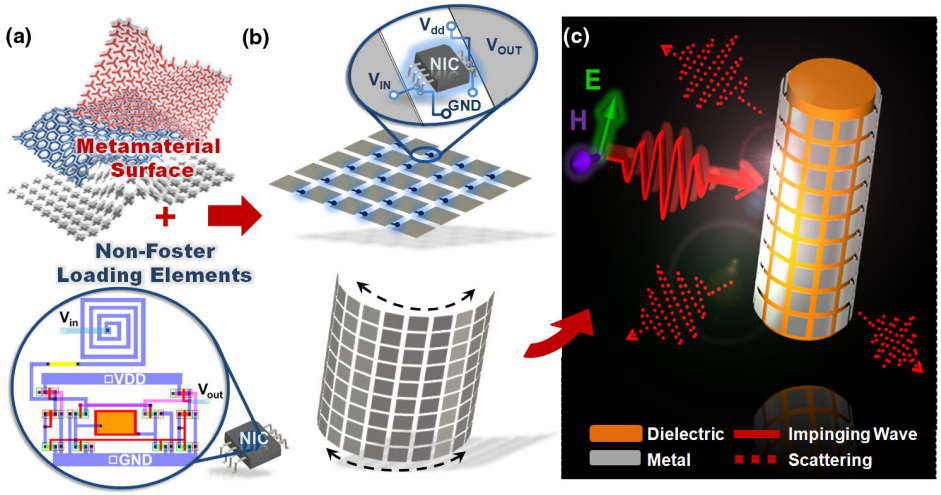

FIG. 1 (color online). Schematics of (a) an ultrathin metasurface formed by structured metal (top) combined with lumped NICs based on complementary metal-oxide-semiconductor technology; (b) assembly of an active non-Foster metasurface; (c) a mantle cloak designed for a dielectric infinite cylinder under TM illumination.

where $\gamma = a/a_c$. This value is inductive for dielectric objects $\varepsilon > 1$, as expected due to the capacitive nature of a moderate size dielectric cylinder. However, the frequency dispersion of the required inductance violates Foster's reactance theorem, which states that the reactance of any passive element in regions of low absorption must monotonically increase with frequency, $\partial X_s(\omega)/\partial\omega > 0$ [31]. Equation actually corresponds to a negative capacitance $Z_s = 1/[-i\omega(-C_{\text{eff}})]$, with $C_{\text{eff}} = \varepsilon_0(\varepsilon - 1)\gamma a/2$, which may be achieved in a circuit only considering amplifiers or active elements, for which Foster's theorem does not apply. Essentially, the metasurface is required to catch up with the capacitive dispersion of the object, requiring an active loading. This is consistent with the idea of relaxing the bandwidth limitations of bulk metamaterials with the use of active inclusions [32]. Indeed, concepts to employ non-Foster elements and active metamaterials to realize broader bandwidths in a variety of applications are being currently explored [33–37].

Even if we may intuitively expect that active inclusions may overcome the passivity constraints mentioned above, in practice it is challenging to design a practical active metamaterial cloak realizing this effect. In the following, on the contrary, we show that a non-Foster mantle cloak may be realistically formed by loading a subwavelength metallic patch array with negative impedance converter (NIC) elements. The mantle cloaking technique is particularly well suited to be combined with lumped NIC elements, and allows combining a large bandwidth of operation with ultralow profile and relatively simple realization.

Moving to the full-wave dynamic scenario, Fig. 2(a) shows the optimal surface reactance $X_{s,\text{opt}}$ (red solid line) required to minimize the total scattering from the dielectric cylinder of Fig. 1 at every frequency point using a lossless mantle cloak with radius $a_c = a$. The curve was calculated using the rigorous analytical formulation developed in [25]: it is obvious that a non-Foster dispersion is indeed required to realize broadband cloaking, as $\partial X_{s,\text{opt}}(\omega)/\partial\omega < 0$ over the whole frequency range of interest. First, let us assume to use a passive mantle cloak with inductive reactance of metasurface (MTS) $-iX_{s,\text{MTS}} = -i\omega L[\Omega]$ and $L = 62.620$ nH, designed to suppress the scattering at the design frequency $f_0 = 0.8$ GHz. Its frequency dispersion (blue solid line) can intersect the optimal reactance curve $X_{s,\text{opt}}$ at one single point $X_{s,\text{FSS}}|_{f_0} = 314.76\ \Omega$, implying that the achievable

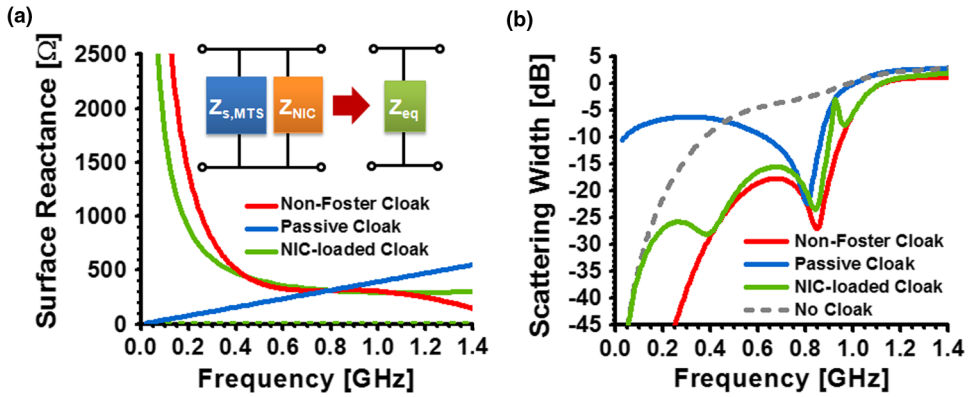

FIG. 2 (color online). (a) Variation of the surface reactance for: an optimal (non-Foster) mantle cloak [red (black in gray scale)], a passive mantle cloak designed to cloak at the design frequency f_0 [blue (gray)], a realistic NIC-loaded [green (light gray)] mantle cloak; the green dashed line shows the corresponding surface resistance. (b) Variation of the normalized SW for the dielectric cylinder covered by the cloaks in (a). The uncloaked scenario (gray dashed) is also shown for comparison.

cloaking bandwidth is intrinsically narrow, as dictated by causality and passivity. Even using a multilayered cloak [2], we may be able to hit the optimal curve at various frequencies, but Foster's theorem would require a scattering peak (pole) to arise in between every two zeros [14,38], inherently limiting the available cloaking bandwidth. Figure 2(b) shows the SW frequency variation for the passive cloaked cylinder (blue solid line), compared to the uncloaked case (gray dashed line). Indeed, the passive cloak can significantly suppress the scattering around the design frequency f_0, but only over a limited bandwidth. Moreover, at lower frequencies, the cloaked cylinder generates more scattering than the uncloaked case, due to its inherent frequency dispersion.

To realize a broadband cloak, we must rely on active metasurfaces that can break Foster's limitations. Our design starts from a passive metasurface made of an array of metal square patches [Fig. 1(b)], with an array period $d = 1.8$ cm and a gap between neighboring elements $g = 0.12$ d. This geometry is well described by the equivalent capacitive impedance $Z^{\mathrm{TM}}_{\mathrm{patch}} = R_{\mathrm{patch}} + 1/(-i\omega C_{\mathrm{patch}})$; detailed expressions for R_{patch} and C_{patch} in terms of the geometry parameters, and their applicability to mantle cloaks, are available in Ref. [26] and the Supplemental Material [39]. When the gaps are loaded by lumped circuit elements Z_{NIC}, as in Fig. 1(a), the equivalent surface impedance is given by the parallel combination of the load impedance and the metasurface impedance [inset of Fig. 2(a)] $Z_{s,\mathrm{eq}} = R_{s,\mathrm{eq}} - iX_{s,\mathrm{eq}} = [(Z^{\mathrm{TM}}_{\mathrm{patch}})^{-1} + (Z_{\mathrm{NIC}})^{-1}]^{-1}$. We consider here active NIC loads connecting neighboring patches, breaking the non-Foster constraints on the surface impedance. The simplest NIC design with such desired functionality is based on a cross coupled pair of transistors [33] (i.e., bipolar junction transistors). However, to be able to tailor $Z_{s,\mathrm{eq}}$ to fit the optimal frequency dispersion $X_{s,\mathrm{opt}}$ over a broad range of frequencies, and at the same time ensuring that the underlying circuit is stable and practically feasible, we propose a system-on-package (SOP) circuit design, including a network of passive, resistive, and reactive components (metasurface). Details of our design layout based on microelectronic technology [Taiwan Semiconductor Manufacture Company (TSMC) 0.18 μm process] are presented in the Supplemental Material [39].

Figure 2(a) shows the calculated surface reactance (green solid line) of our final design, including all parasitic effects expected in the realization of this metasurface. It is seen that the electromagnetic response can be well tailored to follow $X_{s,\mathrm{opt}}$ (red solid line; color online) over a broad frequency range from 0.4 GHz to 1.2 GHz (with a relative error less than 5%). Since our design requirement is to keep the SW below -20 dB, the optimized reactance does not follow $X_{s,\mathrm{opt}}$ at very low frequencies, at which the uncloaked cylinder anyway scatters very little. Figure 2(a) also presents the surface resistance of this active metasurface (green dashed line), verifying that the loss of the proposed non-Foster mantle cloak is small yet positive across all the considered frequency range. This ensures that the scattering response is stable, despite the presence of active elements, and that at the same time, the cloak is reasonably low-loss. In this regard, we stress that we are not aiming here at broadening a resonant response, which may inherently cause stability issues as in recent works on non-Foster impedance matching [40], but instead we suppress the overall scattering of a passive object, which is an inherently nonresonant process, more prone to remain unconditionally stable (see the Supplemental Material [39]). Figure 2(b) shows the corresponding SW for the realistic NIC-loaded mantle cloak (green solid line). The cloak provides a drastically improved bandwidth, much broader than an ideal passive cloak, with a normalized SW well suppressed below -15 dB up to approximately 900 MHz. For very low frequencies, the NIC-loaded mantle cloak does induce slightly more scattering than an ideal non-Foster cloak, but in this region the object itself has a very low scattering signature because of its small electrical size.

Figure 3 shows the calculated far-field scattering patterns for the dielectric cylinder covered by the ideal non-Foster mantle cloak [red line (black in gray scale)], our NIC-loaded mantle cloak [green (light gray) line], and the inductive cloak [blue (gray) line], compared to the uncloaked cylinder (gray shadow) at various frequencies: (a) 0.8 GHz, (b) 0.65 GHz, (c) 0.5 GHz, and (d) 0.4 GHz. In all panels, the scattered fields are plotted in the same scale for fair comparison. It is evident that all cloaks provide excellent scattering suppression at the design frequency f_0 [see Fig. 3(a)]. However, if we observe the far-field scattering away from the design frequency, the passive cloak displays poor performance, compared to the ideal non-Foster or NIC-loaded mantle cloaks. For lower frequencies, a passive cloak induces an even larger scattering than that of the uncloaked dielectric cylinder.

As the frequency increases, the performance of all cloaks deteriorates, due to the excitation of higher-order scattering harmonics, yet the active devices provide improved and more robust performance. The proposed NIC-loaded mantle cloak follows with good agreement the performance of the ideal, optimal mantle cloak, and therefore, provides the best scattering suppression, achievable with a single metasurface over the whole frequency range of interest. Better results, and cloaking for larger objects, aiming at suppressing at the same time multiple scattering harmonics, may be achieved with a multilayer design. The proposed broadband cloak, whose operation covers the entire ultra-high frequency band, may be of particular interest for a wide range of communication applications, beyond camouflaging. Since this technique allows the wave to enter the cloak and interact with the cloaked object, it may enable exciting applications such as broadband cloaked sensing, noninvasive probing [2], and low-interference communications [13].

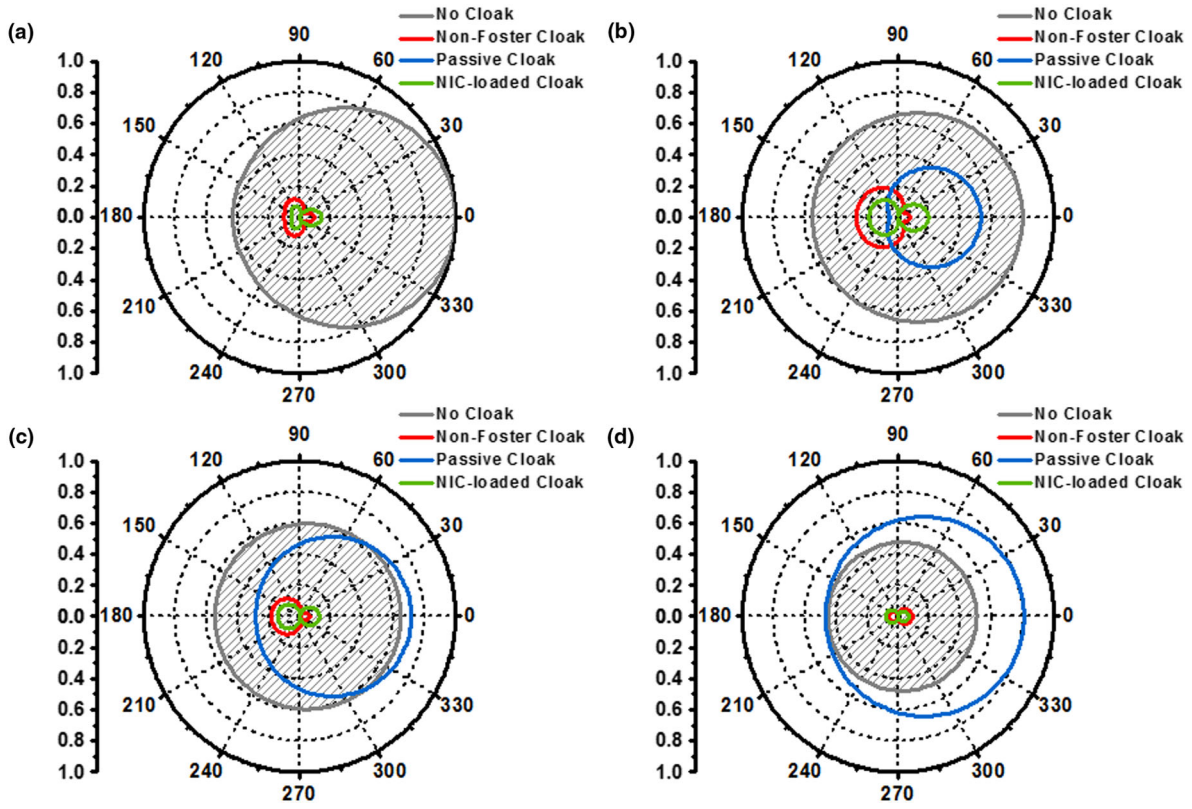

FIG. 3 (color online). (a)–(d) Far-field scattering pattern of the infinite dielectric cylinder without cover (gray shadow), with the ideal non-Foster mantle cloak [red line (black in gray scale)], with the NIC-loaded mantle cloak [green (light gray) line], and with the ideal passive cloak [blue (gray) line], for different frequencies of operation: (a) 0.8 GHz, (b) 0.65 GHz, (c) 0.5 GHz, and (d) 0.4 GHz. In (a), the blue line overlaps the red line, as expected at the central frequency.

We also analyze the time-domain response of the proposed mantle cloaks of Fig. 2 for a short pulse excitation in Fig. 4. This shows how the proposed active device may successfully realize a stable, invisible obstacle for short broadband pulsed excitation. Four receivers are placed in different positions along the z axis, as shown in Fig. 4(a). The distance d_i between the ith receiver or processor $R_{x,i}$ and the origin (center of the cylinder) is $d_1 = -16a$, $d_2 = -6a$, $d_3 = 1.5a$, and $d_4 = 6a$. Therefore, R_1 and R_2 are hit by the impinging signal before the object, whereas R_3 and R_4 are placed behind the object.

Figure 4 shows the calculated transient responses at the different receivers for a short Gaussian pulse with frequency components 0.02–0.9 GHz traveling in free space, comparing the received signals with (solid lines) and without (dashed lines) the cylindrical scatterer. Different scattering scenarios are considered: the uncloaked cylinder [Fig. 4(b)], the NIC-loaded mantle cloak [Fig. 4(c)], and the ideal passive mantle cloak [Fig. 4(d)]. It is seen that the proposed NIC-loaded non-Foster cloak suppresses most of the signal distortion and reflections behind the object. The short pulse shape is restored to the one in absence of the cylinder, both behind and passed the object, implying that its overall bandwidth performance is excellent and stability is

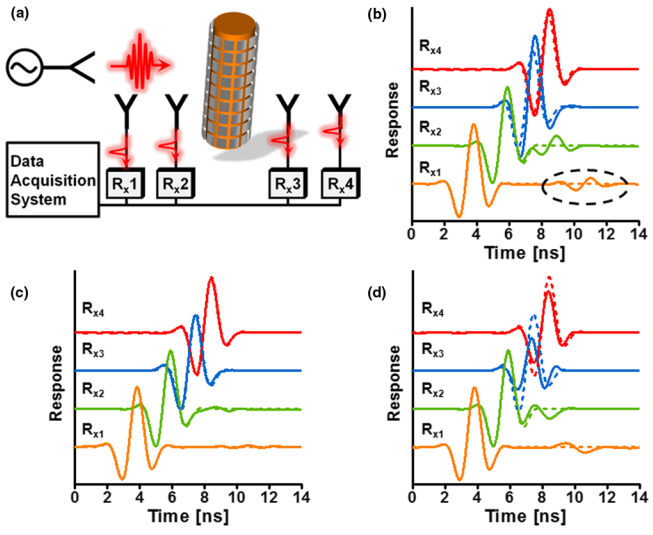

FIG. 4 (color online). (a) Schematic diagram of the time-domain analysis of a cloaked cylinder. Signals are detected by receivers placed in different positions along the z axis, considering the cases of: (b) no cloak, (c) NIC-loaded mantle cloaks, and (d) ideal passive cloak, as in Fig. 2. Here, the transient responses of a short Gaussian pulse traveling in free space (dashed lines) are also shown for comparison.

preserved, despite the active elements in the cloak. Both the uncloaked and the passive cloak, on the contrary, show severely distorted signals, dispersed and delayed in time, as it is particularly obvious for signals received by R_{x1} and R_{x2}. The passive cloak slightly improves transmission, since it cancels the scattering around f_0. However, the remaining frequency components contribute to distorting and stretching the tail and precursor of the signal, due to the relatively narrow cloaking bandwidth. In other words, the passive cloak can be easily detected when excited by a short pulse, while the proposed active cloak has a much more robust performance.

In conclusion, we have proposed here the concept and potential realization of a broadband mantle cloak, formed by a subwavelength metasurface loaded with optimal, active NIC elements. We have demonstrated with both time- and frequency-domain analysis that drastic scattering reduction is achievable over a broad frequency range using an inherently stable, active non-Foster mantle cloak. We envision that this low-profile and broadband cloaking technology may be applied to several applications of interest at rf and microwaves, including camouflaging and invisibility, low-invasive sensing and low-noise communications. We believe that the use of active circuitry in radio frequency cloaks is the ideal route to significantly broaden the cloaking bandwidth and make a significant impact on applications. Even if in this Letter, we specifically focused on mantle cloaks, whose platform is ideal for circuit loading, we expect that exciting effects may be also observed by loading with non-Foster circuit elements other cloaking platforms, such as transformation-based [5] or transmission-line [41] cloaks.

This work was supported by the AFOSR YIP Grant No. FA9550-11-1-0009, the DTRA YIP Grant No. HDTRA1-12-1-0022, and the NSF CAREER Grant No. ECCS-0953311.

[1] A. Alù and N. Engheta, Phys. Rev. E **72**, 016623 (2005).
[2] A. Alù and N. Engheta, Phys. Rev. Lett. **100**, 113901 (2008).
[3] J. B. Pendry, D. Schurig, and D. R. Smith, Science **312**, 1780 (2006).
[4] G. W. Milton and N.-A. P. Nicorovici, Proc. R. Soc. A **462**, 3027 (2006).
[5] D. Schurig, J. J. Mock, B. J. Justice, S. A. Cummer, J. B. Pendry, A. F. Starr, and D. R. Smith, Science **314**, 977 (2006).
[6] U. Leonhardt, Science **312**, 1777 (2006).
[7] B. Edwards, A. Alù, M. G. Silveirinha, and N. Engheta, Phys. Rev. Lett. **103**, 153901 (2009).
[8] H. Chen, B. I. Wu, B. Zhang, and J. A. Kong, Phys. Rev. Lett. **99**, 063903 (2007).
[9] J. Valentine, S. Zhang, T. Zentgraf, E. Ulin-Avila, D. A. Genov, G. Bartal, and X. Zhang, Nature (London) **455**, 376 (2008).
[10] T. Ergin, N. Stenger, P. Brenner, J. B. Pendry, and M. Wegener, Science **328**, 337 (2010).
[11] A. Alù and N. Engheta, Phys. Rev. Lett. **102**, 233901 (2009).
[12] A. Alù and N. Engheta, Phys. Rev. Lett. **105**, 263906 (2010).
[13] A. Monti, J. Soric, A. Alù, A. Toscano, L. Vegni, and F. Bilotti, IEEE Antenn. Wireless Propag. Lett. **11**, 1414 (2012).
[14] F. Monticone, C. Argyropoulos, and A. Alù, Phys. Rev. Lett. **110**, 113901 (2013).
[15] C. Argyropoulos, P. Y. Chen, F. Monticone, G. D'Aguanno, and A. Alù, Phys. Rev. Lett. **108**, 263905 (2012).
[16] F. Monticone, C. Argyropoulos, and A. Alù, Sci. Rep. **2**, 912 (2012).
[17] N. Landy and D. R. Smith, Nat. Mater. **12**, 25 (2013).
[18] H. Chen, Z. Liang, P. Yao, X. Jiang, H. Ma, and C. T. Chan, Phys. Rev. B **76**, 241104 (2007).
[19] F. Monticone and A. Alù, Phys. Rev. X **3**, 041005 (2013).
[20] H. Hashemi, B. Zhang, J. D. Joannopoulos, and S. G. Johnson, Phys. Rev. Lett. **104**, 253903 (2010).
[21] E. Kallos, C. Argyropoulos, Y. Hao, and A. Alù, Phys. Rev. B **84**, 045102 (2011).
[22] A. Alù and N. Engheta, Phys. Rev. E **78**, 045602(R) (2008).
[23] C. Craeye and A. Bhattacharya, IEEE Trans. Antennas Propag. **60**, 3516 (2012).
[24] A. Alù, Phys. Rev. B **80**, 245115 (2009).
[25] P. Y. Chen and A. Alù, Phys. Rev. B **84**, 205110 (2011).
[26] Y. R. Padooru, A. B. Yakovlev, P. Y. Chen, and A. Alù, J. Appl. Phys. **112**, 034907 (2012).
[27] J. C. Soric, P. Y. Chen, A. Kerkhoff, D. Rainwater, K. Melin, and A. Alù, New J. Phys. **15**, 033037 (2013).
[28] B. A. Munk, *Frequency Selective Surface: Theory and Design* (John Wiley and Sons, New York, 2000).
[29] P. Y. Chen and A. Alù, ACS Nano **5**, 5855 (2011).
[30] C. F. Bohren and D. R. Huffman, *Absorption and Scattering of Light by Small Particles* (John Wiley and Sons, New York, 1998).
[31] R. M. Foster, Bell Syst. Tech. J. **3**, 259 (1924).
[32] S. A. Tretyakov, Microw. Opt. Technol. Lett. **31**, 163 (2001).
[33] A. K. S. Hrabar and I. Krois, Metamaterials **4**, 89 (2010).
[34] S. Hrabar, I. Krois, I. Bonic, and A. Kiricenko, Appl. Phys. Lett. **99**, 254103 (2011).
[35] W. Xu, W. J. Padilla, and S. Sonkusale, Opt. Express **20**, 22406 (2012).
[36] S. Hrabar, I. Krois, I. Bonic, and A. Kiricenko, Appl. Phys. Lett. **102**, 054108 (2013).
[37] S. Saadat, M. Adnan, H. Mosallaei, and E. Afshari, IEEE Trans. Antennas Propag. **61**, 1210 (2013).
[38] A. Alù and N. Engheta, New J. Phys. **10**, 115036 (2008).
[39] See Supplemental Material at http://link.aps.org/supplemental/10.1103/PhysRevLett.111.233001 for a surface impedance model of a loaded patch metasurface, practical realization, and stability issues.
[40] E. Ugarte-Munoz, S. Hrabar, D. Segovia-Vargas, and A. Kiricenko, IEEE Trans. Antennas Propag. **60**, 3490 (2012).
[41] P. Alitalo, A. E. Culhaoglu, A. V. Osipov, S. Thurner, E. Kemptner, and S. A. Tretyakov, IEEE Trans. Antennas Propag. **60**, 4963 (2012).